Journal of Nuclear Materials 389 (2009) 326–331

Contents lists available at ScienceDirect

Journal of Nuclear Materials

journal homepage: www.elsevier.com/locate/jnucmat

Study of silver diffusion in silicon carbide

E. Friedland [a,*], J.B. Malherbe [a], N.G. van der Berg [a], T. Hlatshwayo [a], A.J. Botha [b], E. Wendler [c], W. Wesch [c]

[a] Physics Department, University of Pretoria, Pretoria 0002, South Africa
[b] Laboratory for Microscopy and Microanalysis, University of Pretoria, Pretoria, South Africa
[c] Institut für Festkörperphysik, Friedrich-Schiller-Universität, Jena, Germany

A B S T R A C T

Diffusion of silver in 6H–SiC and polycrystalline CVD-SiC was investigated using α-particle channeling spectroscopy and electron microscopy. Fluences of 2×10^{16} cm^{-2} of $^{109}Ag^{+}$ were implanted with an energy of 360 keV at room temperature, at 350 °C and 600 °C, producing an atomic density of approximately 2% at the projected range of about 110 nm. The broadening of the implantation profile and the loss of silver through the front surface during vacuum annealing at temperatures up to 1600 °C was determined. Fairly strong silver diffusion was observed after an initial 10 h annealing period at 1300 °C in both polycrystalline and single crystalline SiC, which is mainly due to implant induced radiation damage. After further annealing at this temperature no additional diffusion took place in the 6H–SiC samples, while it was considerably reduced in the CVD-SiC. The latter was obviously due to grain boundary diffusion and could be described by the Fick diffusion equation. Isochronal annealing of CVD-SiC up to 1400 °C exhibited an Arrhenius type temperature dependence, from which a frequency factor $D_o \sim 4 \times 10^{-12}$ m^2 s^{-1} and an activation energy $E_a \sim 4 \times 10^{-19}$ J could be extracted. Annealing of 6H–SiC above 1400 °C shifted the silver profile without any broadening towards the surface, where most of the silver was released at 1600 °C. Electron microscopy revealed that this process was accompanied by significant re-structuring of the surface region. An upper limit of $D < 10^{-21}$ m^2 s^{-1} was estimated for 6H–SiC at 1300 °C.

© 2009 Elsevier B.V. All rights reserved.

1. Introduction

Fuel elements of modern high-temperature nuclear reactors are encapsulated by CVD-layers which serve as barriers to prevent fission product release. Recent reactor designs generally make use of fuel kernels surrounded by four successive layers of low-density pyrocarbon, high-density pyrocarbon, silicon carbide and high-density pyrocarbon, with silicon carbide being the main barrier for the metallic species. These so-called TRISO particles retain quite effectively most of the important fission products like cesium, iodine, xenon and krypton, but the release of silver seems to present a major problem. Despite the low fission yield of the stable ^{109}Ag (0.03% for ^{235}U) and its low conversion rate of typically 0.1% to ^{110m}Ag by neutron capture, the latter is considered as one of the key fission products. The reason is the high γ-ray dose rate of ^{110m}Ag with a relatively long half-life of 253 days. Release studies from batches of fuel kernels or even entire fuel elements have produced largely differing results concerning magnitude and temperature dependence of silver transport through the particle coatings. While results from earlier investigations could be interpreted as a diffusion process governed by an Arrhenius type temperature dependence [1,2], a recent study found a transport behaviour indicating a flow mechanism through nano-pores [3]. However, a direct comparison of these results makes not much sense, as they were obtained with samples from completely different production sources. In the first case mainly fuel particles from the *Jülich Arbeitsgemeinschaft Versuchsreaktor* (AVR) were investigated, while in the second study *Coorstek* CVD wafers and CVD-diffusion couples prepared at the *Massachusetts Institute of Technology* were analyzed. Most likely the apparently contradictory results can be explained by microstructural differences of the investigated samples.

In order to obtain a better insight in the transport mechanism of silver through CVD silicon carbide layers, one first needs to understand diffusion in single and polycrystalline systems. However, despite various measurements [4,5] no consistent diffusion coefficients for silver are currently available. Published results differ by orders of magnitude. The aim of this study is to obtain information on the importance of volume and grain boundary diffusion through well-defined layers of silicon carbide as well as on the importance of radiation damage for silver transmission. For this purpose silver diffusion in single crystal and in polycrystalline silicon carbide is determined at temperatures up to 1600 °C. The contribution of grain boundary diffusion is estimated by comparing

* Corresponding author. Tel.: +27 12 420 2453; fax: +27 12 362 5288.
E-mail addresses: erich.friedland@up.ac.za, fried@scientia.up.ac.za (E. Friedland).

0022-3115/$ - see front matter © 2009 Elsevier B.V. All rights reserved.
doi:10.1016/j.jnucmat.2009.02.022

the diffusion results of single- and polycrystalline samples. Importance of radiation damage is judged from non-linear effects displayed by isothermal annealing curves.

2. Experimental method

In a series of preliminary experiments silver layers with thicknesses up to a few hundred nano-meters were deposited by vacuum evaporation onto 6H–SiC wafers. These samples were then heated in vacuum to 800 °C for 10 h. Although this temperature is well below the melting point at approximately 960 °C, the deposited layer had completely disappeared due to wetting problems of the silver with the SiC surface. No trace of diffused silver beyond the silicon carbide surface could be detected by either electron microscopy in conjunction with electron diffraction analysis or α-particle backscattering spectroscopy. The diffusion coefficient at this temperature is obviously far below the detection limit of the employed techniques used in this study.

In view of the negative results described in the preceding paragraph, further studies were done with silver implants only. For this purpose 360 keV $^{109}Ag^+$ was implanted in single and polycrystalline SiC wafers with a fluence of 2×10^{16} cm^{-2} at room temperature, at 350 °C and 600 °C. A tilt angle of 7° relative to normal incidence was used to reduce channeling effects. To prevent beam induced target heating, the dose rate was kept well below 10^{13} cm^{-2} s^{-1}. The implanted wafers were vacuum annealed in a computer controlled *Webb 77* graphite furnace for periods ranging from 10 to 80 h at temperatures up to 1600 °C.

The microstructure of the polycrystalline SiC was investigated by field emission scanning electron microscopy (SEM) employing a *Zeiss Ultra 55* instrument fitted with an electron backscattering diffraction (EBSD) detector. The EBSD technique was used to determine the polytypes of the grains of the CVD-SiC wafers. Depth profiles were obtained by Rutherford backscattering spectrometry (RBS) at room temperature using α-particles with energies between 1.4 and 1.8 MeV. The same set-up was also used to investigate radiation damage in the single crystalline samples by channeling spectroscopy employing a three-axes precision goniometer. The analyzing particle beam was collimated at a spot of 1 mm diameter and the current of approximately 10 nA was measured directly on the target. A ring-shaped electrode in front of the target was kept at a negative potential of 200 V to suppress secondary electrons. Sufficient counting statistics was obtained by collecting an integrated charge of 8 μC. Backscattered particles were observed at either 165° or 170° by a surface barrier detector telescope with an acceptance angle of 2°. Aligned spectra were normalized to random spectra collected during rotation of the sample about an axis tilted by approximately 5° relative to the channeling direction. Energies of the backscattered particles are converted to a depth scale by using the energy loss data of Ziegler [6]. Depth resolution near the surface is limited by the system's energy resolution of 12 keV to approximately 15 nm for α-particles scattered from silver atoms. Because of energy straggling this value increases to almost 20 nm at a depth of 100 nm.

3. Results

A typical implantation profile is shown in Fig. 1 together with a simulation obtained with the TRIM-98 code [7] assuming displacement energies of 35 eV and 20 eV for the silicon and carbon atoms, respectively [8]. The experimentally observed projected range of 108 nm is in good agreement with the theoretical estimate of 106 nm, but range straggling is about 26% larger than predicted. The kurtosis (β) and skewness (γ) of the distribution is almost Gaussian ($\beta = 3$; $\gamma = 0$). Fick's diffusion equation for the dilute limit leads to a particularly simple solution if the original profile at time

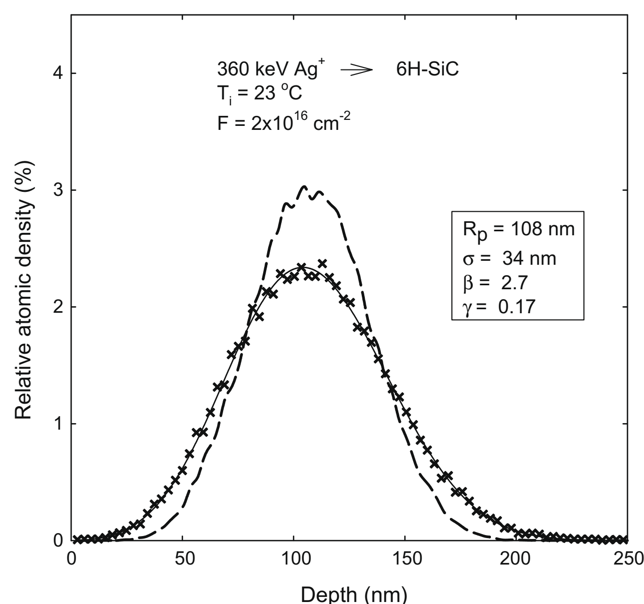

Fig. 1. Silver depth profile in 6H–SiC as determined by RBS. The broken line is the theoretical distribution obtained with the TRIM-98 code [7].

$t_0 = 0$ can be described by a Gaussian distribution [9]. In that case the concentration profile after annealing for a time t stays a normal distribution in an infinite medium and is given by

$$C(x,t) = K[\pi Dt]^{-1/2}\exp(-x^2/4Dt).$$

In this equation K is an adjustable constant, while the position of the maximum concentration is unchanged at $x = 0$. Defining the profile width $W(t)$ as the full width at half maximum (FWHM), the following relationship between the final and original widths holds:

$$[W(t)]^2 = 4Dt\ln(2) + [W(0)]^2.$$

Hence the slope of a plot of $[W(t)]^2$ versus annealing time at constant temperature will directly yield the diffusion coefficient D.

As-implanted channeling spectra for cold and hot implantations are depicted in Fig. 2. Arrows indicate the surface positions of silicon and silver. The surface position of carbon is at channel 110. As is to be expected for the applied high fluence, which introduces a total displacement damage of almost 50 dpa at a depth of 80 nm, complete amorphization up to a depth of approximately 260 nm is obtained at room temperature. However, implantation at 600 °C caused no amorphization with the crystal structure largely preserved. The broad peak around channel 240 is mainly due to lattice distortions caused by the implanted silver atoms. Backscattering yield from a small amount of tungsten evaporated from the heater coil onto the sample is observed at channel 485. Similar results are found for implantations at 350 °C. The radiation hardness of SiC above 300 °C has been previously reported for other heavy ions [10].

3.1. Polycrystalline silicon carbide

In this study CVD-SiC wafers, purchased from *Valley Design Corporation*® were used. A cross-sectional SEM image is shown in Fig. 3. It reveals that the material consists mainly of columnar crystallites aligned along the growth direction with diameters of a few micrometers. However, it shows also smaller crystals not parallel to the columns. EBSD analysis indicated that the lattice structure is mainly cubic, but that some hexagonal growth modes are also present. The long thin columnar crystals exhibit numerous planar

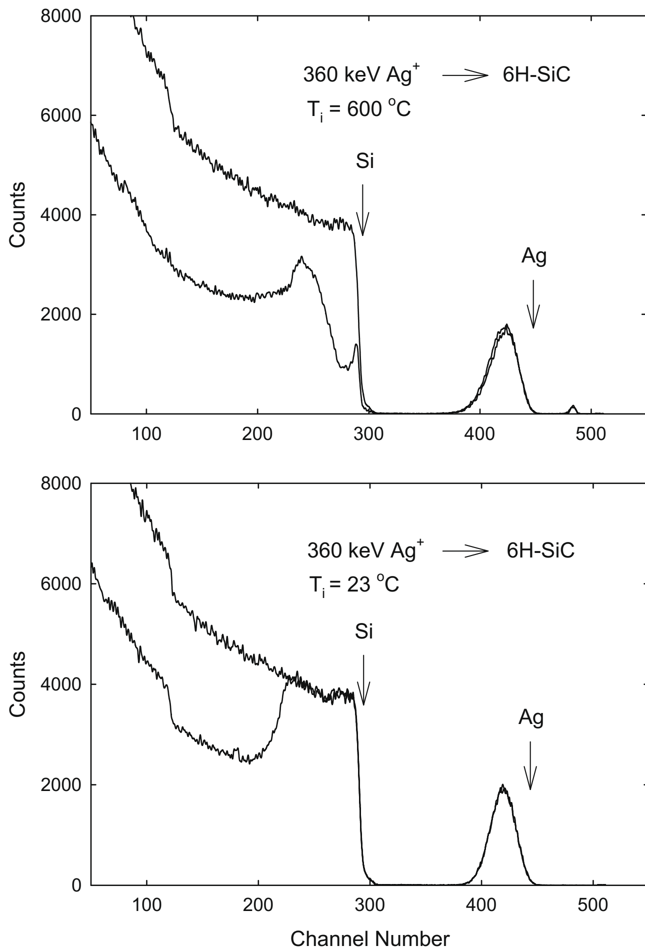

Fig. 2. Aligned and random α-particle backscattering spectra of silver implants in 6H–SiC at room temperature and 600 °C. The energy of the analyzing beam was 1.4 MeV and the scattering angle 170°.

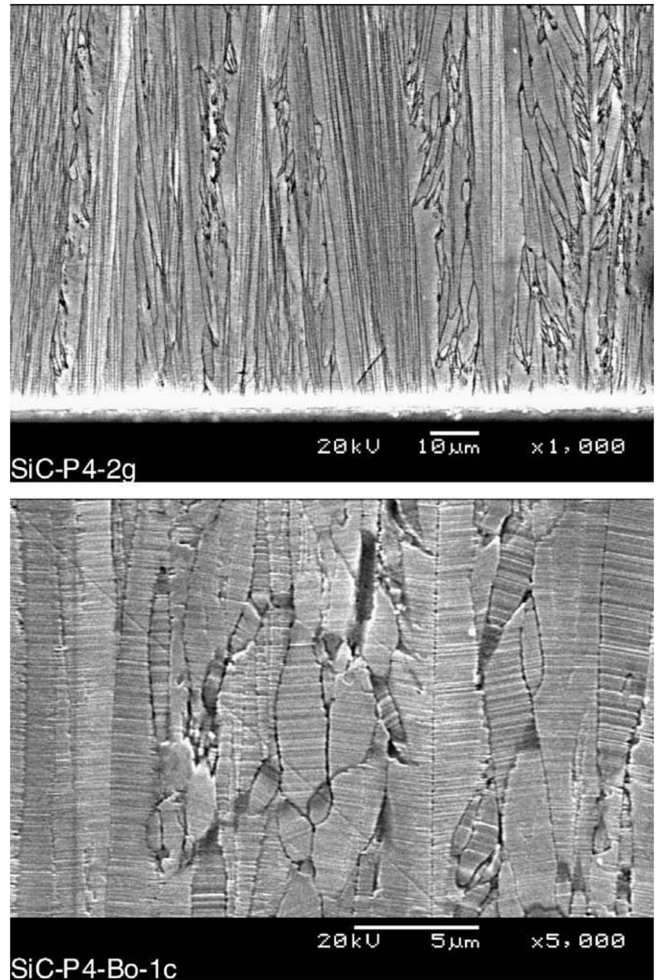

Fig. 3. A polished and etched cross-sectional SEM image of a polycrystalline SiC sample, showing a columnar structure in the growth direction, which coincides with the implantation direction.

defects, while twinning occurs frequently. Fig. 4 is a SEM image of the top surface, showing clusters of small crystals surrounded by larger crystals, which form the columnar structure. The surface of this image is also the surface through which the implantation was done.

Silver transport in the implanted wafers was investigated by isochronal and isothermal annealing experiments. For the isochronal study samples were sequentially annealed for 10 h at temperatures of 800 °C, 900 °C, 1100 °C, 1200 °C, 1300 °C, 1400 °C and 1450 °C. Depth profile broadening started to appear after the 1200 °C heating cycle. At 1300 °C the profile reached the surface and a slight loss of silver was observed, while more than 25% of it was lost after annealing at 1400 °C. Fig. 5 shows some of the depth profiles for a sample implanted at 350 °C.

A temperature of 1300 °C was chosen for the isothermal annealing investigation, because the rate of profile broadening is reasonably large at that temperature, while silver loss from the surface is still acceptable. Measured widths of the silver profiles after annealing between 10 and 80 h are plotted in Fig. 6. An outstanding feature is the relatively sharp increase during the first annealing cycle, while further annealing increases the profile width at a much lower but constant rate.

3.2. Single crystalline silicon carbide

Hexagonal 6H–SiC wafers obtained from *Intrinsic Semiconductors®* were used for isochronal and isothermal annealing studies of single crystalline samples. A preliminary annealing for 2 h at 960 °C of a sample implanted at room temperature caused an epitaxial re-growth from the bulk to reduce the amorphous surface region from 260 nm to about 220 nm. The implanted silver layer at R_p = 106 nm was therefore still in the disordered silicon carbide region and its depth profile had not changed significantly. Fig. 7 shows the depth profiles after further annealing for 10 h each at 1500 °C and 1600 °C. In contrast to the polycrystalline case, no broadening is observed. Instead a shift to the surface occurs, accompanied with an increasing loss of silver from the surface. From the shape of the distribution it is quite obvious, that no detectable diffusion into the bulk takes place. Channeling spectroscopy shows furthermore that during the last annealing step the surface region has completely been re-grown epitaxially, although the residual defect density is quite high.

As with the polycrystalline sample, isothermal annealing studies were done at 1300 °C. The results are depicted in Fig. 8. Again a rather sharp increase of the width occurs after the first annealing cycle of 10 h, but further heat treatment does not change the width of the silver depth profile any further.

4. Discussion

The relatively large broadening of the silver profiles after the first annealing period at 1300 °C in both the poly- and single crystalline samples is without any doubt due to implantation

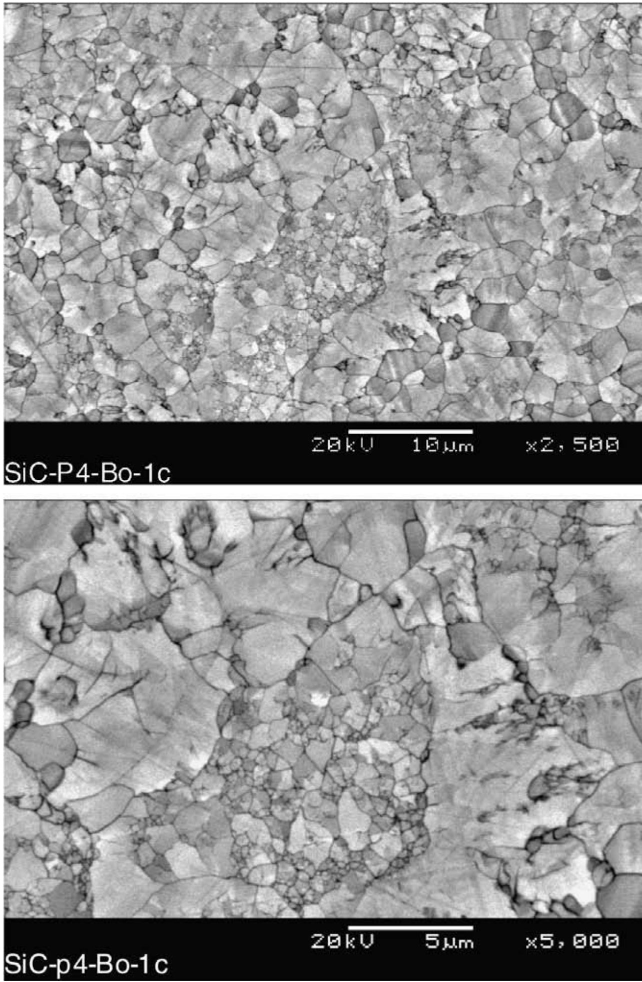

Fig. 4. SEM image of the etched top surface of a CVD-SiC wafer, which is also the surface through which the implantation was done.

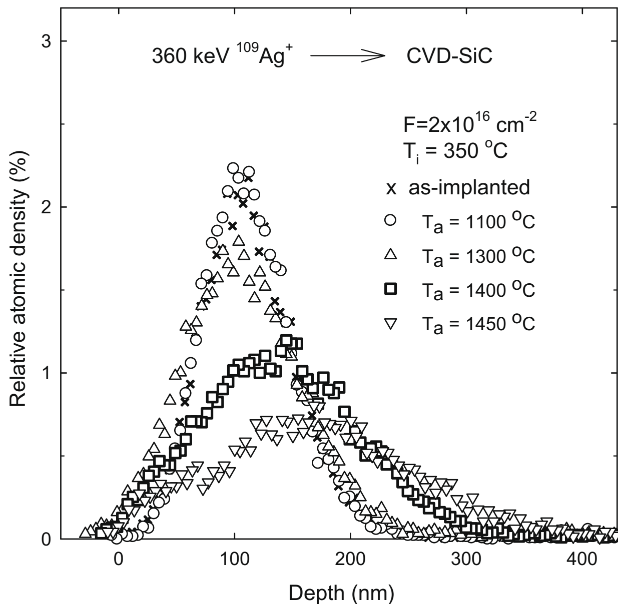

Fig. 5. Silver depth profiles in CVD-SiC after isochronal annealing for 10 h for a sample implanted at 350 °C.

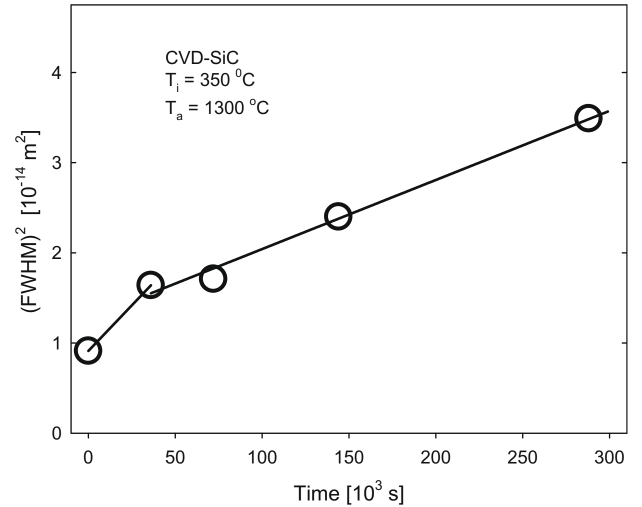

Fig. 6. Square of the full width at half maximum (FWHM) of the silver profile in CVD-SiC as a function of the isothermal annealing time at $T_a = 1300$ °C. From the slope a diffusion coefficient $D \sim 3 \times 10^{-20}$ m^2 s^{-1} is extracted.

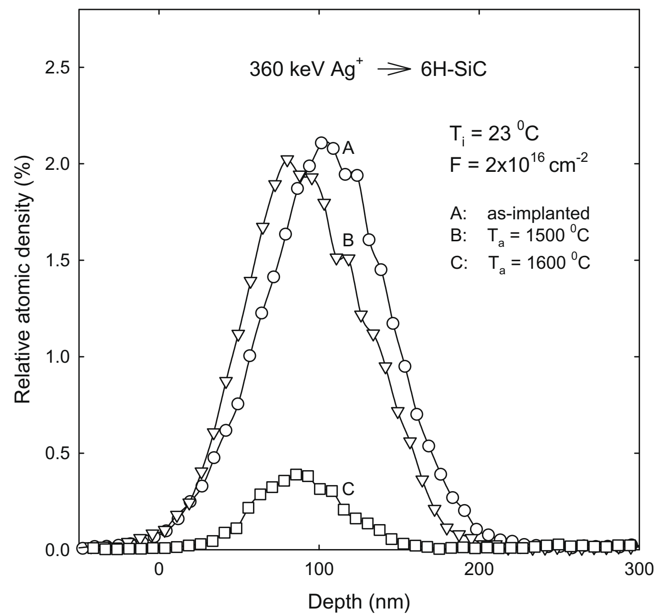

Fig. 7. Silver depth profiles in 6H–SiC implanted at room temperature after isochronal annealing for 10 h.

induced radiation damage. In the case of the 6H–SiC, which was implanted at room temperature, the silver was initially embedded in amorphous silicon carbide, while in the CVD-SiC it was surrounded by polycrystalline matter containing a relatively high density of extended defects. From the initial slopes effective diffusion coefficients could be calculated. This, however, would be a rather meaningless exercise as the structural evolution of the material during this first annealing stage is not quantified. The only conclusions one can draw is that diffusion is enhanced in defective or amorphous SiC and that most of the damage annealing occurring at this temperature is completed after 10 h. A reduced but linear profile broadening was observed in the polycrystalline sample after the first annealing cycle, while in the single crystalline material no further broadening was observed within experimental error. From the linear relationship one can deduce that Fickian diffusion conditions prevail after the initial annealing step. The diffusion

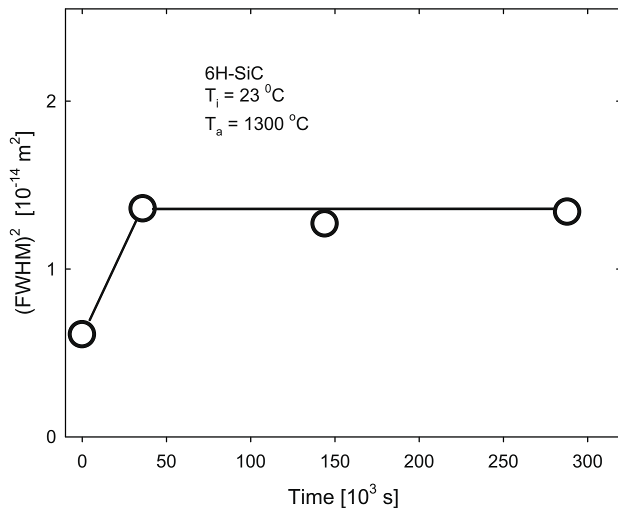

Fig. 8. Square of the full width at half maximum (FWHM) of the silver profile in 6H–SiC as a function of the isothermal annealing time at T_a = 1300 °C. From the slope an upper limit of the diffusion coefficient $D < 10^{-21}$ cm^2 s^{-1} is extracted.

coefficients obtained from fitting the experimental data for $t > 10$ h to a straight line yields

$$D_{CVD} = (2.8 \pm 0.2) \times 10^{-20}\,\text{m}^2\,\text{s}^{-1} \quad \text{and}$$
$$D_{6H} < 10^{-21}\,\text{m}^2\,\text{s}^{-1} \quad \text{at} \quad 1300\,^\circ\text{C}.$$

The upper limit for the single crystalline SiC is reconcilable with the result of Ref. [5], who found at 1500 °C a value of $D < 5 \times 10^{-21}$ m^2 s^{-1}. In view of this extremely low limit the diffusion in CVD-SiC can almost entirely be associated with grain boundary diffusion. A rough estimate from Fig. 5 of the relatively small fraction of grain boundary area exposed at the top surface shows that grain boundary diffusion must be many orders of magnitude larger than volume diffusion. The quoted statistical error is obtained for a particular sample. As the diffusion depends on the random distribution of grain sizes, differences between individual samples are significantly larger. At 1300 °C variations of up to 50% were found for diffusion coefficients of different samples cut from the same wafer. Our result is in variance with the findings of Ref. [5], who observed no sign of silver migration via either inter- or intra-granular paths. It is known that free silicon is often stored at grain boundaries and a trace of it was detected in our samples by X-ray diffraction analysis. Silver and silicon do not form a silicide, but a melt of Ag–Si alloy coexists with solid silicon above 840 °C [11], which can provide diffusion paths for silver. In view of the observed low silicon concentration it is unlikely that this mechanism plays an important role in our measurements, although this cannot be excluded with certainty.

Poly- and single crystalline samples were subjected to isochronal annealing cycles of 10 h each, starting at 800 °C and increasing the temperature between each cycle by initially 100 °C and above 1400 °C by 50 °C. Some of the obtained depth profiles are shown in Figs. 5 and 7 for poly- and single crystalline samples, respectively. In the case of CVD-SiC the first measurable broadening was observed at 1200 °C. Up to 1400 °C the shape of the profiles were approximately Gaussian, allowing an analysis in terms of the procedure discussed above. At 1450 °C the silver loss through the surface was excessive and the profile turned highly skewed towards the bulk, which rendered an analysis unreliable. Diffusion coefficients varied between 1.41×10^{-20} cm^2 s^{-1} at 1200 °C and 1.46×10^{-19} cm^2 s^{-1} at 1400 °C. Assuming Arrhenius type temperature dependence, a theoretical fit of the experimental data yielded the following values for the frequency factor and activation energy:

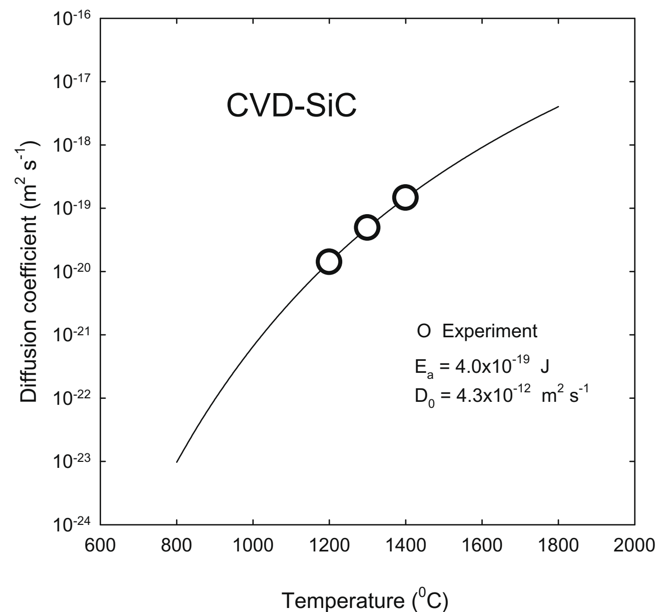

Fig. 9. Experimental silver diffusion coefficients (O) in CVD-SiC. The solid line represents a theoretical fit assuming Arrhenius type temperature dependence.

$$D_o = (4.3 \pm 0.2) \times 10^{-12}\,\text{m}^2\,\text{s}^{-1}$$

and

$$E_a = (4.0 \pm 0.1) \times 10^{-19}\,\text{J}.$$

Concerning the quoted experimental errors, a similar qualifying remark as made before is again applicable. The results plotted in Fig. 9 can be accommodated with those of Ref. [4], who found no diffusion in a similar experiment after annealing at 1180 °C for 30 min. According to the above result the diffusion coefficient at that temperature is approximately 10^{-20} m^2 s^{-1} and the expected profile broadening after such a short annealing time would be difficult to detect by RBS analysis.

As mentioned before, no diffusion in 6H–SiC was observed up to 1600 °C. Instead a shift of the profile towards the surface accompanied by a simultaneous loss of silver occurs above 1450 °C. This is in agreement with the observations of Ref. [12], who found no evidence of silver diffusion in single crystalline SiC at temperatures up to 1300 °C but a tendency of the silver to shift towards the surface at higher temperatures. SEM images show at these temperatures significant structural changes of the surface region. Fig. 10 is an image showing re-crystallization and island formation as well as possible silver segregation after annealing at 1400 °C. This may indicate the start of a sublimation process, which could easily explain the observed phenomenon. However, it must be borne in mind, that the structural changes may be a result of the presence of silver, and might not necessarily occur in pure SiC.

5. Conclusion

The results prove that silver diffusion in single crystalline silicon carbide is extremely low up to 1600 °C as long as the stability of the material is guaranteed. In polycrystalline silicon carbide diffusion along grain boundaries has to be taken into account at temperatures above 1100 °C. At the typical maximum temperature of 1000 °C encountered inside a fuel kernel of a gas-cooled high-temperature nuclear reactor, the diffusion coefficient of CVD-SiC samples studied in this work would be less than 10^{-21} m^2 s^{-1}. Intact silicon carbide coatings of typically 35 μm thicknesses in

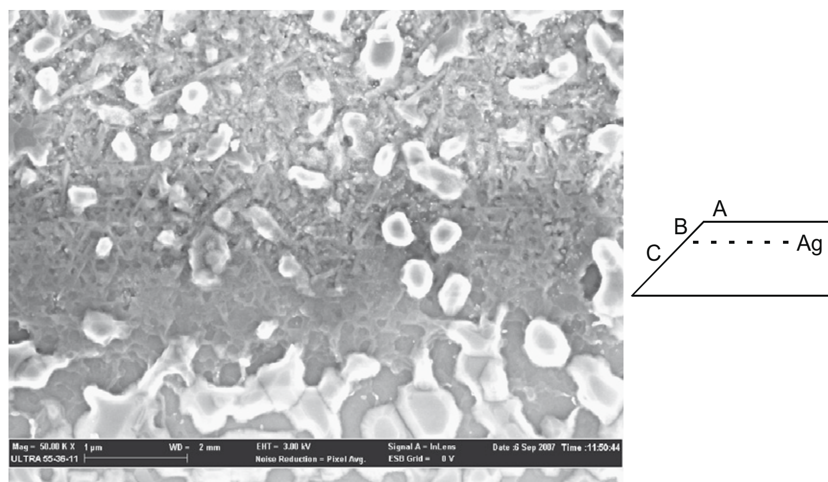

Fig. 10. SEM image of a 6H–SiC sample after annealing for 10 h at 1400 °C showing re-crystallization and island formation. The sample was polished at an angle of 135° as shown schematically in the included sketch. Zone A represents the top surface, zone B the cross-sectional area containing the implanted silver and zone C the unimplanted SiC. The magnification bar represents 1 μm.

fuel kernels should therefore effectively prevent silver release into the reactor's primary cooling system during their total resident time in the core. The fact that significantly higher effective diffusion coefficients have been determined in silver release studies must therefore be either due to SiC coatings containing diffusion enhancing impurities in their grain boundaries or structural imperfections like cracks or pores.

Acknowledgements

Financial support of this study by PBMR (Pty) Ltd. of the Republic of South Africa is gratefully acknowledged.

Thanks are due to Johan de Villiers from the *Department of Material and Metallurgical Science*, *University of Pretoria*, for the X-ray diffraction analyses and to Gerald Lenk from the *Institut für Festkörperphysik, Friedrich-Schiller-Universität Jena*, for the silver implantations.

References

[1] W. Amian, Experimentelle Untersuchung zum Transportverhalten von Silber in Brennstoffteilchen für Hochtemperaturreaktoren, KFA-Jülich, Jül-1731, Jülich, 1981.
[2] W. Amian, D. Stöver, Nucl. Technol. 61 (1983) 475.
[3] H.J. MacLean, Silver Transport in CVD Silicon Carbide, PhD Thesis, MIT, Department of Nuclear Engineering, 2004.
[4] H. Nabielek, P.E. Brown, P. Offermann, Nucl. Technol. 35 (1977) 483.
[5] H.J. MacLean, R.G. Ballinger, L.E. Kolaya, S.A. Simonson, N. Lewis, M.E. Hanson, J. Nucl. Mater. 357 (2006) 31.
[6] J.F. Ziegler, The Stopping and Ranges of Ions in Matter, Pergamon, New York, 1977.
[7] J.F. Ziegler, J.P. Biersack, U. Littmark, The Stopping and Ranges of Ions in Solids, Pergamon, New York, 1985.
[8] R. Devanathan, W.J. Weber, F. Gao, J. Appl. Phys. 90 (2001) 2303.
[9] S.M. Myers, S.T. Picraux, T.S. Prevender, Phys. Rev. B 9 (1974) 3953.
[10] E. Wendler, A. Heft, W. Wesch, Nucl. Instrum. and Meth. B 141 (1998) 105.
[11] F.A. Shunk, Constitution of Binary Alloys, McGraw-Hill Company, New York, 1969.
[12] W. Jiang, W.J. Weber, V. Shutthanandan, L. Li, S. Thevuthasan, Nucl. Instrum. and Meth. B 219/220 (2004) 642.